Proceedings of the ASME 2010 3rd Joint US-European Fluids Engineering Summer Meeting and 8th International Conference on Nanochannels, Microchannels, and Minichannels
FEDSM-ICNMM2010
August 1-5, 2010, Montreal, Canada

FEDSM-ICNMM2010-30948

FLUID STRUCTURE INTERACTION EXCITING MECHANISMS OF FLEXIBLE STRUCTURES IN UNIFORM FLOWS

Jorge Pereira Gomes and Hermann Lienhart
Institute of Fluid Mechanics and Erlangen Graduate School in Advance Optical Technologies
Friedrich-Alexander University of Erlangen-Nuremberg
Cauerstrasse 4, D-91058 Erlangen, Germany
Email: jgomes@lstm.uni-erlangen.de; hermann.lienhart@lstm.uni-erlangen.de

ABSTRACT

The oscillation of a structure immersed on a flow can become self-excited as a result of different fluid-structure interaction mechanisms. To identify the self-exciting mechanisms and to understand the influence of the physical parameters on the different exciting processes, the two-dimensional free swivelling movement of flexible structure models were investigated in both laminar and turbulent uniform flows.

The coupled fluid and structure movement was characterized using a particle image velocimetry (PIV) system complemented by a time-phase detector to obtain accurate time-phase resolved measurements of the flow velocity field and structure deformation. The experimental tests proved that the self-exciting mechanisms are strongly dependent on the approaching flow velocity. For the velocity range tested, a sequence of clearly defined movement-induced excitation (MIE) and instability-induced excitation (IIE) of the model was observed on increasing the velocity of the incoming flow.

In this contribution, the results for one specific structure configuration are presented.

NOMENCLATURE

A' Fluid mass.
B Structure damping.
B' Fluid damping.
C Structure stiffness.
d Structure characteristic length.
f_N Structure natural frequency.
m Structure mass.
n Order of the frequency harmonic.
St Strouhal number.
T Structure swivelling period.
t Delay of the measurement to the beginning of the cycle.
tpa Time-phase angle: $\text{tpa} = (t/T) \times 360°$.
U Approaching flow velocity.
y Position along the y-direction.
ζ Structure damping coefficient.
ω_N Angular frequency associated to f_N: $\omega_N = 2\pi f_N$.

INTRODUCTION

The excitation, and posterior amplification, of a structure and fluid oscillating system can be described, in a first approach to the problem, as follows. If a structure deforms, its orientation to the flow changes and it determines a change in the fluid forces acting upon the surface of the structure. A new set of fluid forces determines a new structure deformation. As soon as this coupled mechanism is initiated, as a result of any initial flow or movement instability, the damping imposed by the fluid can become negative as a result of different mechanisms by which energy is transfered from the fluid to the structure. Whether the excited oscillation is damped out or amplified is just a matter of the sign of the net damping coefficient. For lightly damped structures, the fluid damping becomes dominant and the coupled fluid and structure movement may become self-excited. Depending on the role of the fluctuation of the flow in the initial excitation process, the excitation is either called extraneously-induced excitation (EIE), instability-induced excitation (IIE) or movement-induced excitation (MIE) [1, 2].

In the case of EIE, the fluctuations are produced by an extraneous source. Therefore, the exciting frequency is independent of the structure movement and controls the frequency of the resulting oscillation. Excitation mechanisms of this kind induce the structure to undergo forced-oscillations.

In opposition to EIE, IIE is caused by an instability of the flow which gives rise to flow fluctuations if a certain threshold value of flow velocity is reached. As a rule, this instability is intrinsic to the flow created by the structure and exists even in those cases in which structure oscillations do not occur. An example of flow instability is the alternate vortex shedding formation in the wake behind a bluff body. Depending on the control and amplification mechanism affecting the instability, these fluctuations and the forces they generate can become well correlated and close to a dominant frequency of the mechanical oscillator, in this way they can lead to large-amplitude movements of the oscillating system. Thus, this type of excitation is expected to occur in a finite small range of flow velocities in which the flow fluctuation is in resonance with the first or higher harmonics of the natural frequencies of the structure [3]. This corresponds to the condition

$$\frac{U}{f_N d} \approx \frac{1}{nSt} \; . \tag{1}$$

In the resonance range of limited amplitude, it is expected no changes in the dynamical characteristics of the structure movement because it is reasonable to assume that the fluid stiffness balances the added mass.

Excitation of the type MIE is characterized by fluctuating forces that arise from the movement of the structure. Whenever the structure is accelerated in the fluid, an unsteady flow is induced that alters the fluid forces acting upon the structure. If this alteration in the fluid load leads to a negative damping or to a transfer of energy to the moving structure, a MIE process starts. In this process, the forces that are responsible for the excitation are inherently linked to the structure movement and disappear if the structure comes to rest. In other words, the exciting fluid forces have components in phase with the acceleration and with the velocity of the structure, respectively. The sensitivity of the oscillating system to MIE can be described by the equation of movement

$$\left(m+A'\right)\ddot{y}\left(t\right)+\left(B+B'\right)\dot{y}\left(t\right)+Cy\left(t\right)=0 \; , \tag{2}$$

where A' and B' are known as added, or fluid coefficients and account for the effects of the fluid. The criterion for dynamic instability with respect to infinitesimal disturbances can be stated in terms of the net damping of the system as

$$2\zeta m\omega_N + B' \leq 0 \; . \tag{3}$$

Regarding the behavior of the added mass, it can be seen from equation (2) that A' is not zero at the onset of MIE. Thus, in opposition to IIE, an influence on the dynamics of the structure in the case of MIE is expected.

Regardless the excitation mechanism, the self-excitation onset and resulting oscillation movements are very difficult to predict whenever the structure has a complex geometry or multiple degrees-of-freedom (such as flexible structures). From the numerical research view point, the challenges with respect to mathematical modeling, numerical discretization, solution techniques, and their implementation as software tools on modern computer architectures are still huge, in particular if accuracy, flexibility and simulation efficiency are considered. An overview of the present development of numerical solution strategies and their applications can be found in [4, 5].

The recent developments in new numerical methodologies triggered the present work to perform an experimental research in the field of FSI to investigate the instability and the resulting FSI induced swivelling motion of complex flexible structures immersed in uniform laminar and turbulent flows. The object of the research were two-dimensional structure models which combine the elastic behavior of a flexible sheet in an axial flow with the dynamic of a prism in cross-flow.

The selection of the experiments and the detailed measurements performed during the present work primarily aimed to identify the different fluid-structure interaction self-exciting mechanisms and to understand the influence of the physical parameters on the different exciting processes. The parameters involved the incoming fluid characteristics and the geometric and mechanical properties of the structure. The study also investigated both laminar and turbulent flow regimes, to account for the influence of the Reynolds number on the self-exciting process. To control the Reynolds number and the flow velocity independently, the viscosity of the test liquid was modified during the tests. Second, the experimental investigation addressed the need for experimental data on reference test cases. It provided a reliable data base on specific, well-defined reference test cases to be used as a diagnostic and validation tool for numerical models for fluid-structure interaction simulations.

The identification of the self-exciting mechanisms was performed after the characterization of the general character of the elastic-dynamic response of the structure model as a function of the approaching flow velocity. Then, the analysis of the resulting structure movement for each individual excitation mechanism was performed on the trace of the structure body angle, trailing edge coordinates, structure deformation and flow velocity field.

In the present contribution, the results obtained for a specific structure models are presented. They include the elastic-dynamic response of the structure and the characterization of the resulting swiveling movement for the most significant swiveling-modes. The results concerning the flow velocity field are not discussed in the present text.

EXPERIMENT DEFINITION

The present contribution presents the results obtained for the flexible structure shown in figure 1. In addition to well defined linear mechanical properties, this model has proved to satisfy the requirements for periodicity and reproducibility of the resulting flow and structure motion for both laminar and turbulent regimes. It consisted of a $0,04$ mm thick stainless steel sheet attached to an 22 mm $\times$ 8 mm rectangular stainless steel front body. At the trailing edge of the flexible sheet a 10 mm $\times$ 4 mm rectangular stainless steel mass was located. All the structure was free to rotate around an axle located in the central point of the front body. Both the front body and the rear mass were considered rigid. The flexible section of the structure has proven to have a linear mechanical behavior within the range of forces acting on it during the tests and the Young modulus was measured to be 200 kN/mm^2. The overall span-wise dimension of the structure was chosen to be 177 mm to match the dimensions of the test section and consequently to guarantee the two-dimensionality of the movement.

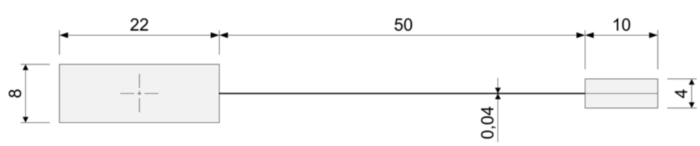

FIGURE 1. STRUCTURE MODEL GEOMETRY [mm].

The tests were conducted in a vertical, closed loop tunnel in two different liquids. For the investigation in the laminar regime, a polyethylene glycol syrup at a controlled temperature of $25^\circ \pm 0,5^\circ$ was used as the test fluid. Within this temperature range, the mixture could be considered incompressible and Newtonian; its kinematic viscosity and density were measured to be constant at $1,64 \times 10^{-4}$ m^2/s and 1050 kg/m^3, respectively. On the other hand, the tests in turbulent flows were conducted in water at the temperature of 22° C. The test section had an overall length of 338 mm and a cross section area equal to 180 mm $\times$ 240 mm. The structure was mounted 55 mm downstream of the inlet plane of the test section on ball bearings, therefore, the rotational degree of freedom of the structure could be considered to be free of friction. Opting for a vertical tunnel, the gravity force was aligned with the x-axis and so it did not introduced any asymmetry. The experiment domain of the tests is represented in figure 2.

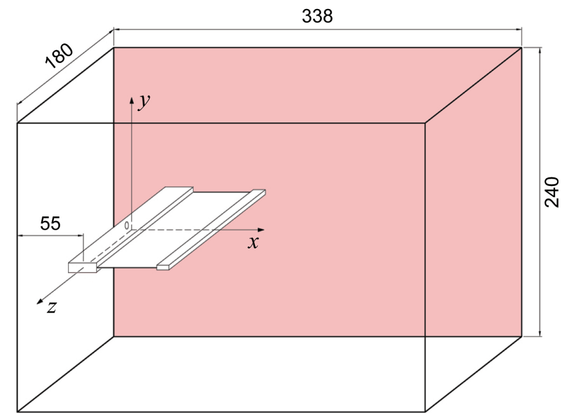

FIGURE 2. TEST SECTION GEOMETRY [mm].

The measurements aimed to characterize both the unsteady movement of the structure and the surrounding fluid flow. The task of measuring the two-dimensional flow field around the model was performed using particle image velocimetry (PIV) technique.

To determine the position of the structure model and consequently to reconstruct its elastic-dynamic response, the PIV system was modified to provide it with structure deflection analysis capabilities. The idea behind this set-up was to use the PIV system to acquire images from the swiveling structure and to use an especially developed software to analyze and reconstruct the time-dependent deformation of the structure. The PIV cameras were now located in such a way to acquire images of the flexible structure illuminated by the laser sheet from each side of the model. No seeding was used during these tests. The quantitative analysis was performed after images acquisition in Matlab workspace by a script developed for the specific task. The software analyzed and compared the images of both sides of the model and reconstructed the time dependent image of the light sheet reflected by the structure. To achieve that purpose it mapped the pixel value in the gray-scale of the entire image and detected the line resulting from the intersection of the laser sheet and the structure as well as the edges of the rear mass. With the information of the position of the flexible sheet all relevant data of the deflected structure could be computed.

Because all the investigation was based on free-oscillating tests, cycle-to-cycle fluctuations of the resulting coupled unsteady flow and structure motion time period were registered. To cope with these fluctuation and to resolve the measurements in the time-phase space, an in-house designed time-phase detector was implemented to obtain accurate time-phase resolved measurements. The idea was to operate the system at constant acquisition rate and both events, the acquisition of a measurement and the start of a new movement cycle, recorded based upon an absolute clock. Using this time information, the data was reorganized in a post-processing program to provide the time-phase resolved data. The time-phase detector was developed with an internal 1 Mhz clock to provide a detection accuracy of 2μs. During the tests two signals were detected and recorded: the internal triggering signal of the cameras to indicate the instant of the measurement and the signal of a magnetic angular position sensor connected to the structure to indicate the beginning of a new swiveling cycle. Thus, the measurements were reconstructed introducing the time-phase angle tpa = $(t/T) \times 360°$; the time-phase angle of 0° and 360° correspond to the beginning and end of a the swiveling motion period, respectively. More detailed description of the measurement techniques is given elsewhere [6, 7].

RESULTS

The structure model was first tested at different approaching flow velocities up to 2 m/s in the laminar regime. Figures 3 and 4 show the elastic-dynamic response of the structure as a function of the flow velocity. The Reynolds number of the experiments, based on the overall length of the model, reached the maximum value of 1000 at 2 m/s.

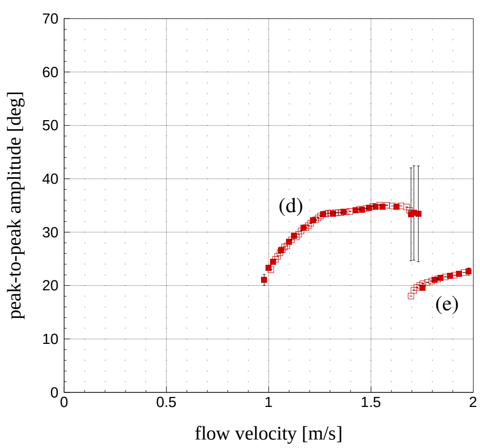

FIGURE 3. STRUCTURE MOVEMENT AMPLITUDE VERSUS FLOW VELOCITY IN LAMINAR REGIME.

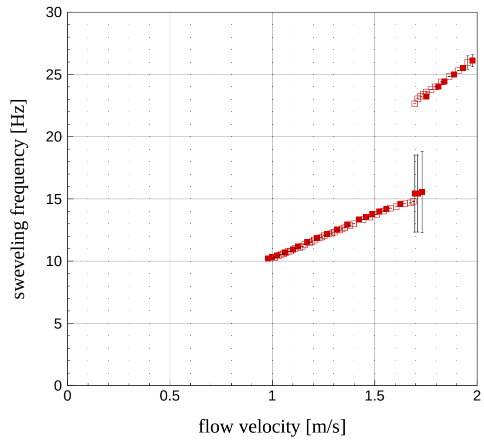

FIGURE 4. STRUCTURE SWIVELLING FREQUENCY VERSUS FLOW VELOCITY IN THE LAMINAR REGIME.

The most obvious aspect revealed by the figures was the existence of two distinctive swivelling-modes. The figures also indicated that at low flow velocities, it was not possible to identify any kind of motion. On increasing the flow velocity, it was observed that the velocity threshold to excite the movement of the structure was very close to 1 m/s. At this velocity, the excitation was abrupt and no transient could be measured. According to visualizations performed at different flow velocities, this swivelling-mode [(d), figure 3] was characterized by the fact that the deformation of the structure model was predominantly dominated by the structure second bending-mode. In connection with this, the movement of the rear mass was in opposition with the rotation of the front body. These observations were confirmed by detailed measurements performed at $1,45$ m/s. At this velocity, the Reynolds number was equal to 725, and the frequency of the resulting structure swivelling movement was measured to be equal to $11,22$ Hz $\pm 0,4\%$. Figure 5 shows the time-phase trace of the front body angle and the transverse displacement of the structure trailing edge within a period of motion. The curves in the figure indicate that the movement of the trailing edge was in opposition, but delayed, in respect to the rotation of the front body. This delay was measured, as time-phase angle, to be approximately 95°. The standard deviation associated to the measurement of the angle was equal to $0,4°$. In figure 6, the deformation of the structure for successive instants within a period of motion is shown. In this figure, the uncertainty associated to the structure deformation was estimated to be equal to $0,2$ mm, approximately.

The other swiveling-mode was registered for velocities higher than $1,7$ m/s. The transition occurred at constant velocity and it was characterized by a discontinuity in both movement amplitude and frequency. This swiveling mode [(e), figure 3] was characterized by the fact that the rear mass movement was in accordance to the rotation of the structure front body. At the same time, higher bending-modes, in particular the structure third bending-mode, were registered to have a decisive contribution to the deformation of the structure.

To support the analysis of this swiveling mode, a similar set of measurements were performed at $1{,}92$ m/s, which corresponded to a Reynolds number equal to 960. At this velocity, the frequency of the structure movement was measured to be equal to $25{,}36$ Hz. Figure 7 shows the time-phase trace of the front body angle and the y-coordinate of the structure trailing edge within a period of motion.

The results showed a degradation of the periodicity and reproducibility of the movement of the structure within this swivelling-mode. To support this statement is the fact that the standard deviation associated to the swivelling motion frequency and front body angle were measured to be equal to $1{,}9\%$ and 1°, respectively. These values were about the double of the values found during the tests at lower velocities. In adition, the movement of trailing edge was registered to be in accordance to the movement of the front body, with a delay of about 65°, measured as time-phase angle. The deformation of the structure for successive time-phase angles within a period of motion is displayed in

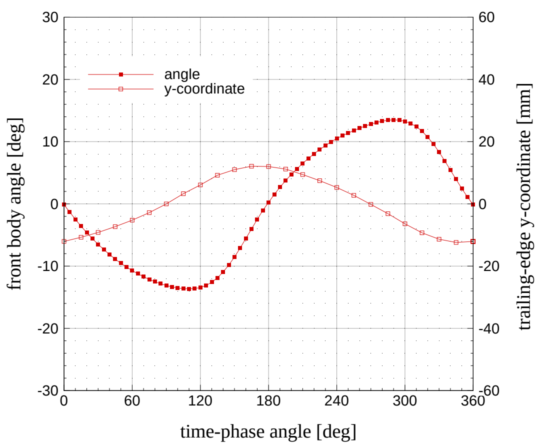

FIGURE 5. STRUCTURE FRONT BODY ANGLE AND TRAILING EDGE Y-COORDINATE WITHIN A PERIOD OF MOTION AT $1{,}45$ m/s ($Re = 725$).

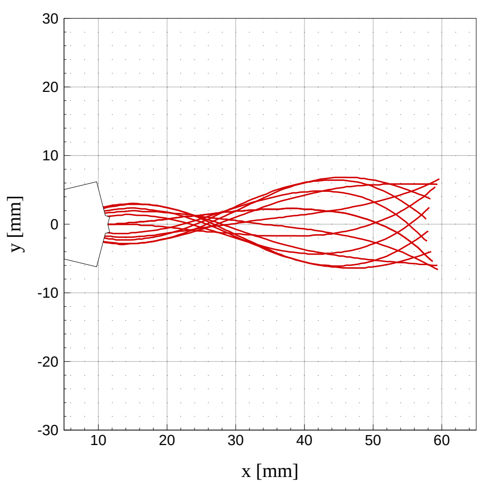

FIGURE 6. TIME-PHASE RESOLVED STRUCTURE DEFORMATION WITHIN A PERIOD OF MOTION AT $1{,}45$ m/s ($Re = 725$).

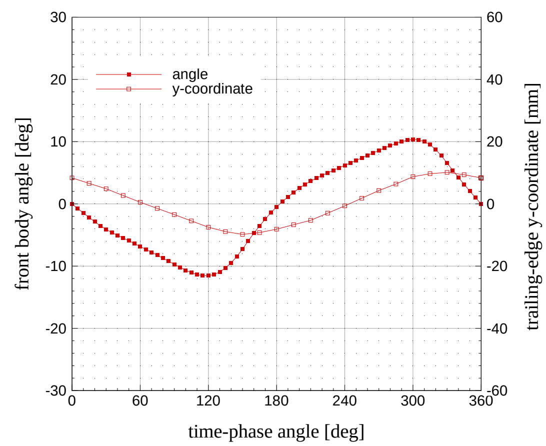

FIGURE 7. STRUCTURE FRONT BODY ANGLE AND TRAILING EDGE Y-COORDINATE WITHIN A PERIOD OF MOTION AT $1{,}92$ m/s ($Re = 960$).

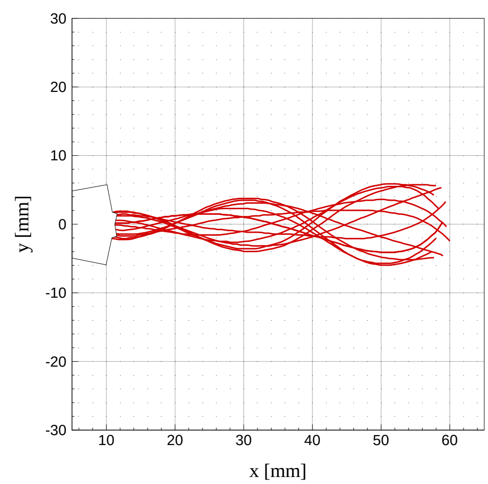

FIGURE 8. TIME-PHASE RESOLVED STRUCTURE DEFORMATION WITHIN A PERIOD OF MOTION AT $1{,}92$ m/s ($Re = 960$).

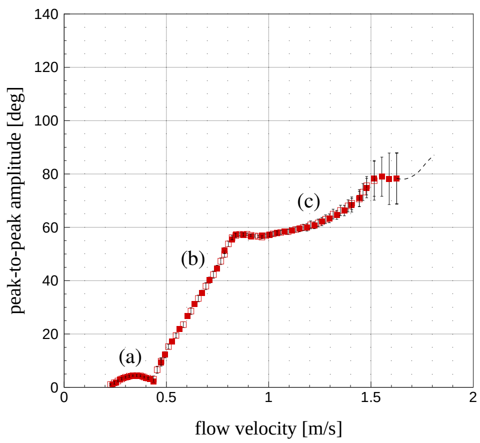

FIGURE 9. STRUCTURE MOVEMENT AMPLITUDE VERSUS FLOW VELOCITY IN THE TURBULENT REGIME.

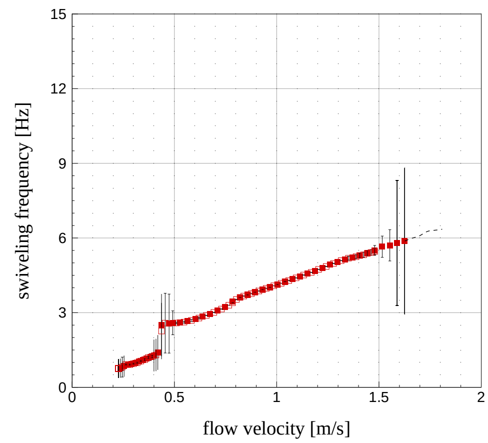

FIGURE 10. STRUCTURE SWIVELLING FREQUENCY VERSUS FLOW VELOCITY IN THE TURBULENT REGIME.

figure 8. The existence of two pronounce nodal regions in the collection of deformations in the figure clearly shows the influence of the third bending-mode in the deformation of the structure within the excitation of this swiveling-mode. The cycle-to-cycle fluctuation of the structure position has proved to be similar to the one measured in figure 6. Therefore, the same uncertainty of $0,2$ mm should be considered for these results.

In the turbulent regime, using water as the working fluid, the structure proved to have the same well-defined multi-swiveling mode behavior as observed in laminar flows. Figures 9 and 10 present the elastic-dynamic response of the structure versus the water flow velocity up to $1,7$ m/s. At this maximum velocity, the Reynolds number of the experiments achieved the maximum value of 143600.

This time, the structure was excited to a periodic swiveling motion at very low flow velocities. In addition, three different swiveling-modes were identified as a function of the flow velocity. The lowest swivelling-mode [(a), figure 9] could be excited for flow velocities at about $0,2$ m/s and it was mostly characterized by a weak oscillation of the structure; the maximum excitation was observed at $3,5$ m/s at the same time that the deflection of the front plate was limited to $\pm 2,1^\circ$. Although the movement of the structure could not be considered as a pure rigid body movement, visualizations at different flow velocities have proved that the deformation of the structure was minimal and that the structure mostly behaved like a pendulum.

Around $0,43$ m/s, a transition to a new swivelling mode was observed. It occurred when the structure was in resonance with its zero natural frequency, $f_0 = 1,9$ Hz, and it was characterized by a significant cycle-to-cycle fluctuation of the frequency. From the movement amplitude view point, no fluctuations were registered. During the excitation of the this swivelling-mode [(b), figure 9] , the elastic-dynamic response of the present structure has proved to be as simple as possible. The amplitude of the movement varied linearly with the flow velocity and the deformation of the structure was almost exclusively dominated by the structure model first bending-mode. In agreement to this fact, the movement of the trailing edge was observed to be in accordance to the rotation of the rectangular front body.

To better characterize this swiveling-mode, figure 11 shows the time-phase trace of the rectangular front body angle and y-coordinate of the structure trailing edge within a period of motion for an approaching velocity of $0,68$ m/s. At this velocity, the Reynolds number was equal to 57500, and the frequency of the structure motion was measured to be equal to $2,87$ Hz $\pm 1\%$.

The two curves in figure 11 indicate that the movement of the trailing edge was in accordance with respect to the rotation of the front body. The time-phase delay was measured to be approximately 75° and the standard deviation associated to the measurement of the front body angle was equal to $0,6^\circ$. In figure 12 the deformation of the structure for successive time-phase angles is displayed for a movement period.

At about $0,8$ m/s, a significant change in the elastic-dynamic response curve in figure 9 was registered indicating that a new self-exciting mechanism was competing for the control of the structure movement and forcing a mode transition. The new swivelling-mode [(c), figure 10] was concluded to be more complex and the character of the structure movement has proved to be unique in comparison to all the other swivelling-modes measured to this point. These observations were followed by investigations of the structure movement at different flow velocities within the range from $0,9$ m/s to $1,4$ m/s and, in particular, by detailed measurements performed for a constant approaching velocity equal to $1,22$ m/s. In figures 13 and 14, the characterization of the structure movement at this velocity is shown. The Reynolds number was defined to be equal to 103100 and the frequency of the structure movement was measured to be equal to $4,71$ Hz $\pm 1\%$.

Figure 13 shows the time-phase trace of the front body angle and the transverse displacement of the structure trailing edge within a period of motion. The movement of the trailing edge was registered to stay in accordance to the rotation of the front body, with a time-phase delay of about 60°, and the standard deviation associated to the angle in the figure was equal to $0,6^\circ$.

In figure 14, the structure deformation for successive time-phase angles within a movement period is shown.

They were conclusive to indicate that this swivelling-mode possessed the main characteristics of a swiveling-mode dominated by the first bending-mode of the structure. This conclusion was supported by the fact that the deformation of the structure was in general very similar to the deformation observed within the previous swivelling-mode. The comparison between figure 14 and figure 12 makes the last statement very clear. The only significant difference revealed by the figures is related to the amplitude of the movement and it shows that the movement of the structure at $1,22$ m/s is wider than at $0,68$ m/s.

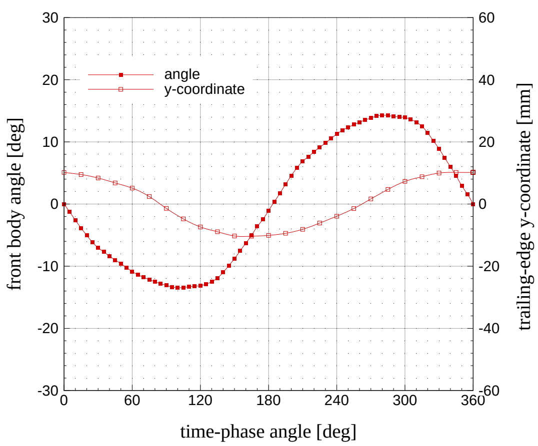

FIGURE 11. STRUCTURE FRONT BODY ANGLE AND TRAILING EDGE Y-COORDINATE AT $0,68$ m/s ($Re = 57500$)

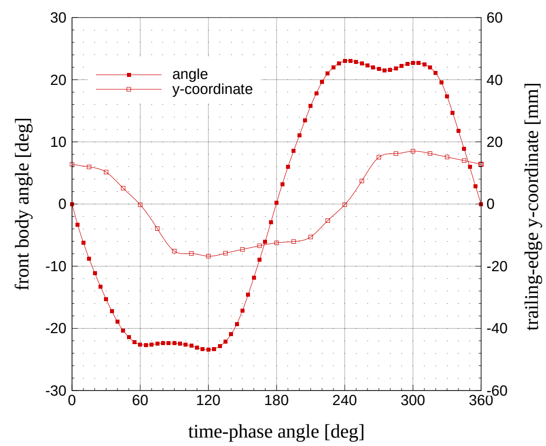

FIGURE 13. STRUCTURE FRONT BODY ANGLE AND TRAILING EDGE Y-COORDINATE AT $1,22$ m/s ($Re = 103100$).

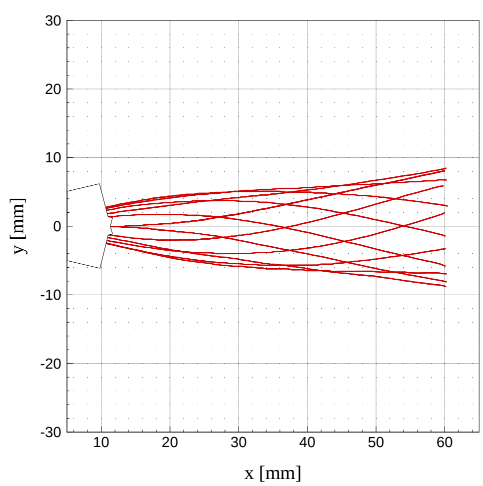

FIGURE 12. TIME-PHASE RESOLVED STRUCTURE DEFORMATION WITHIN A PERIOD OF MOTION AT $0,68$ m/s ($Re = 57500$).

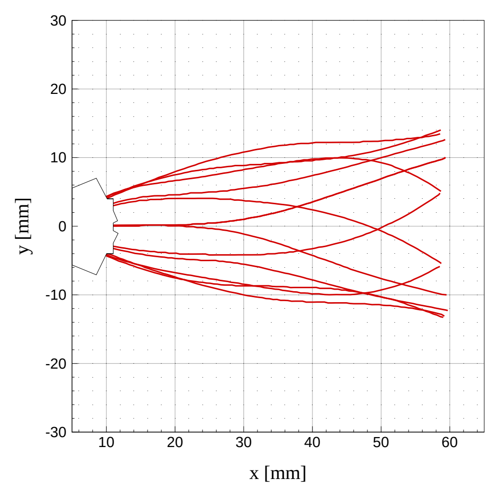

FIGURE 14. TIME-PHASE RESOLVED STRUCTURE DEFORMATION WITHIN A PERIOD OF MOTION AT $1,22$ m/s ($Re = 103100$).

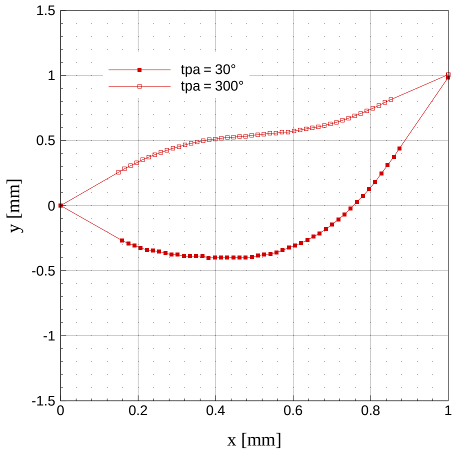

FIGURE 15. NORMALIZED STRUCTURE DEFORMATION FOR TPA=30° AND TPA=300° AT 1,22 m/s ($Re = 103100$).

But when figure 14 is analyzed in more detail, it becomes evident that higher bending-modes rather than just the first one are controlling the deformation of the structure. The influence of the first bending-mode to the deformation of the structure is better seen at the time phase-angle equal to 30° while the influence of higher modes, in particular the second swivelling-mode, is better seen at tpa=300°, see figure 15. In this figure, the deformations of the structure were normalized to the unity in order to improve the comparison between the two curves. In summary, figures 14 and 15 show that this swivelling-mode was not predominantly dominated by a single bending-mode, but by the first and second bending-modes. This shared control of the structure deformation justify the unique characteristics of the present swivelling-mode. Among the unusual features, the trace of the front body angle was characterized by a "figure-of-M" shape in which two positive and two negative local maximums were clearly identified, see figure 13. On the other hand, the shape of the of the trailing edge trajectory no longer assumed the "figure-of-eight" as observed for all the previous swiveling-modes and structure models but exhibited two singular points where the it was observed a sudden reverse in the direction of the movement.

On further increasing the velocity of the flow, the structure movement became non-symmetric and non-periodic. This rapid succession of events which resulted in the destruction of the model close to 1,8 m/s, happened at the same time that the frequency of the structure model was close to its first natural frequency, $f_1 = 5,61$ Hz. During the tests in turbulent flows, the cycle-to-cycle fluctuation of the structure position was observed to be slightly bigger than the one in the laminar regime. This increased the uncertainty associated to the deformation measurements in both figures 12 and 14 to 0,33 mm.

DISCUSSION OF THE RESULTS

In the laminar regime, it was possible to distinguish two swiveling-modes depending on the approaching flow velocity. For both modes, the structure movement frequency increased linearly with the flow velocity while the front body movement amplitude presented local maximums.

The lower swivelling-mode could only be excited at a flow velocity very close to 1 m/s and the it was characterized by having two local maximums, at approximately 1,27 m/s and 1,55 m/s. For the velocity of the first local maximum, the corresponding laminar Strouhal number and the second natural frequency of the structure, $f_2 = 27,45$ Hz, revealed a strong interconnection between the excited movement and the classical von Karman vortex shedding triggered by the structure front body. In respect to the deformation of the structure, this swiveling-mode was mostly dominated by the structure second bending-mode. This conclusion was supported by the pronounced node observed in the structure deformation and later confirmed by the decomposition of the results in the model bending-mode shape functions.

The transition to the higher, faster swiveling mode was registered around 1,7 m/s and it was characterize by a significant cycle-to-cycle fluctuation of the movement parameters. Within this swiveling-mode, the frequency of the structure movement was much lower than the third natural frequency of the structure model, $f_3 = 92,75$ Hz, indicating a self-exciting mechanism of a different type than the previous one. Despite a small delay, the trailing edge movement was in phase with the movement of the rectangular front body. The analysis of the structure deformation results revealed that the deformation of the structure was mainly dominated by the third-bending mode. Its dominance resulted in the pronounced two node registered in the deformation of the structure.

One may observe that none of the self-excited swiveling-modes was directly associated to the first natural frequency of the structure. If any structure movement have happened as a consequence of an exciting process involving this frequency, it would have occurred for a flow velocity smaller then 1 m/s. The absence of any result within this range of velocities was a direct consequence of the high damping imposed by the test fluid which inhibited the amplification of any structure oscillation around the critical velocity corresponding to $f_1 = 5,61$ Hz.

In the turbulent regime, three different swiveling-modes were observed within the flow velocity range up to 2 m/s. The lowest one started at a very small flow velocity and it was characterized by small movement amplitudes and frequencies. The amplitude of the structure front body reached the maximum value of ±2,1° at 0,35 m/s. In a similar way as for the first laminar swiveling-mode observed, a direct connection between the movement excitation and the classical von Karman vortex shedding behind the structure front body was proven to exist, based on the first natural frequency of the structure, f_1, and the turbulent Strouhal number. This fact justified the minimal but noticeable deformation of the structure observed during visualizations performed within this swiveling-mode.

The first swiveling-mode transition was registered at about $0,43$ m/s. The new mode was characterized by the fact that the amplitude of the movement increased monotonically with the approaching flow velocity. The trailing edge was observed to be almost in phase in relation to the front body rotation and the analysis of the deformation revealed that the movement of the structure was just defined by the first bending-mode of the structure model. The same direct relation between the movement excitation and the classical von Karman vortex shedding was observed for this swiveling-mode on comparing the Strouhal number and the first harmonic of the first natural frequency of the structure, $2f_1$.

Finally, at $0,8$ m/s the structure started to give indications of a second swivelling-mode transition. The resulting swivelling-mode was more complex and difficult to understand. The trace of the front body angle presented a unique "figure-of-M" shape indicating that the structure models changed the direction of the movement six times within a period of motion. In connection to this, the figure described by the structure trailing edge (not shown in the present contribution) no longer corresponded to the classical "figure-of-eight" as observed for all the others swiveling-modes but presented two singular points. The analysis of the structure deformation revealed that the structure movement was still dominated by its first bending-mode but with a strong influence of the second. The active presence of the second swiveling-mode could be easily understood seeing that this swiveling-mode occurred for flow velocities around the critical velocity associated to the second natural frequency, f_2. In sum, for this self-excited swiveling-mode it was not possible to draw a direct relation between the excited movement and the vortex shedding.

Beyond $1,5$ m/s it was not possible to register the elastic-dynamic behavior of the structure. On increasing the velocity, the resulting movement of the model became unstable and non-reproducible, finally leading to the failure of the structure.

Finally, one may discuss the excitation of the first bending-mode at low Reynolds numbers.

The critical velocity given by expression (1) is very small for the first natural frequency of the structure, f_1, and this constituted one of the main factors for the damping of the excitation. In order to force an excitation associated to f_1, the critical velocity was increased by increasing the characteristic length of the structure. Figure 16 shows a model consisted of a aluminium circular front body with the same dynamic characteristics of the model presented in figure 1. The only difference between the two is the shape of the front body. All the other mechanical properties, including the momentum of inertia of the model around the free rotating axle, where identical. Thus, one can conclude that the structures in figures 16 and 1 have the same natural frequencies.

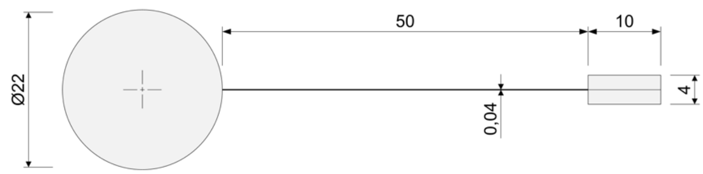

FIGURE 16. CIRCULAR FRONT BODY STRUCTURE MODEL GEOMETRY [mm].

Figure 17 represents the movement amplitude of this structure as a function of the approaching flow velocity. The figure shows that the onset of the first swiveling-mode [(f), figure 17] was registered between $0,75$ m/s and $0,8$ m/s.

An identical analysis as performed for the previous swivelling-modes, based on these velocity values and on the correspondent laminar Strouhal number revealed a direct connection between the classical von Karman vortex shedding and the first natural frequency of the structure, $f_1 = 5,61$ Hz.

In figure 18 the deformation of the circular front body structure is represented for successive time-phase angles within a period of motion at $1,07$ m/s. The figure concludes that the resulting structure movement as similar in nature to the one registered in figure 12. In both cases, the structure movement resulted from the self-excitation of the first bending-mode of the structure model.

Just to make the description of figure 17 complete, within the second swiveling-mode [(g), figure 17] the movement of the structure was mostly dominated by the second bending-mode of the structure model.

CONCLUSIONS

The results of the structure elastic-dynamic response proved the existence of different structure swivelling-modes both in laminar and turbulent flow regime.

The comparison of the results was not very easy because none of the swivelling-modes was repeated in the results. In the laminar regime, the structure first bending-mode failed to be self-excited at small velocities because of the high damping imposed by the fluid whereas in turbulent flows the structure model failed before having the opportunity to excite the structure second and third bending-modes. Nevertheless, one may conclude that the lower swivelling-modes in both flow regimes [(a) and (b), figure 9, and (d), figure 3] were triggered by the vortex shedding created around the front body. Considering all evidences, it can be concluded that these swivelling-modes correspond to

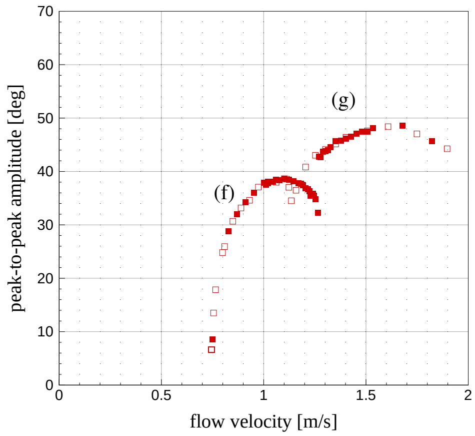

FIGURE 17. STRUCTURE MOVEMENT AMPLITUDE VERSUS FLOW VELOCITY IN THE TURBULENT REGIME, CIRCULAR FRONT BODY STRUCTURE.

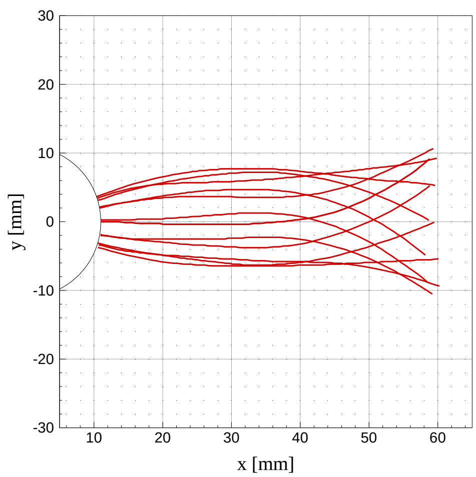

FIGURE 18. TIME-PHASE RESOLVED STRUCTURE DEFORMATION WITHIN A PERIOD OF MOTION AT 1,07 m/s, CIRCULAR FRONT BODY STRUCTURE.

IIE fluid-structure interaction cases. The excitation processes responsible for the higher swivelling-modes [(c), figure 9, and (e), figure 3] were more difficult to examine. However, the results strongly indicate that these modes can be attributed to MIE. In particular, the first one corresponds to MIE involving mode-coupling.

As far as the structure first bending-mode in laminar flows is concerned, its excitation could just be achieved with a thicker circular front body structure model. This result tend to prove that the excitation of the first bending-mode in the laminar regime for the rectangular front body structure was not possible because the correspondent critical velocity was bellow the velocity threshold need to amplify the flow instabilities which gives rise to flow fluctuations and consequently to an excitation of the type IIE. In the case of the circular front body structure, the critical velocity associated to f_1 was bigger and the amplification found favorable conditions to happen. For similar reasons as for the rectangular front body structure, this swivelling-mode corresponded to an excitation mechanism of the IIE type.

ACKNOWLEDGMENT

The authors gratefully acknowledge the support given by the German Science Foundation (DFG) - Germany - and Fundação para a Ciência e a Tecnologia (FCT) - Portugal - to the present study and also the funding of the Erlangen Graduate School in Advanced Optical Technologies (SAOT) by DFG.

REFERENCES

[1] Naudascher E., Rockwell D., 1980, ”Oscillator-model approach to the identification and assessment of flow-induced vibrations in a system”, Journal Hydraulics Research, **18**, pp.59-82

[2] Naudascher E., Rockwell D., 2005, *Flow-induced Vibrations*, Dover

[3] Sarpkaya T., 1978, ”Fluid forces on oscillating cylinders”, Journal of the Waterway Port Coastal and Ocean Division, **WW4**, pp.275-290

[4] Souli M., Hamdouni A., eds., 2007, ”Fluid structure interaction: Industrial and Academic Applications”, European Journal of Computational Mechanics, **16**, pp.303-548

[5] Hartmann S., Meister A., Schäfer M., Turek S., eds., 2009, *Fluid-structure interaction: Theory, numerics, applications*, Kassel University Press

[6] Gomes J. P., Lienhart H., 2006, ”Time-phase resolved PIV/DMI measurements on two-dimensional fluid-structure interaction problems”, *International symposium 13th Int Symp on Applications of Laser Techniques to Fluid Mechanics*, 16. - 29. June, Lisbon

[7] Gomes J. P., Lienhart H., 2006, ”Experimental Study on a Fluid–Structure Interaction Reference Test Case”, *Fluid-Structure Interaction, Lecture Notes Comput. Sci. & Eng., LNCSE*, Springer, Vol. **53**, pp.356-370